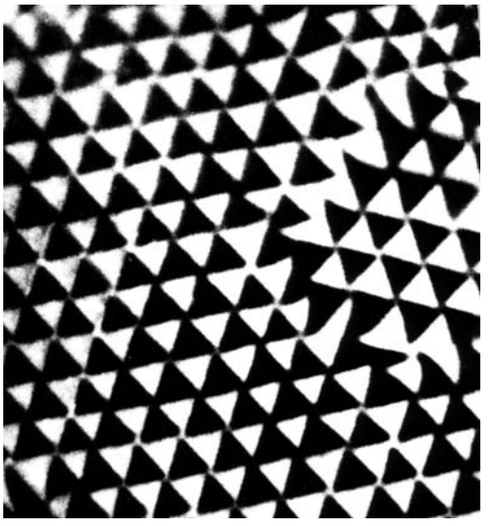

Fig. 3.4.4.5. Transmission electron microscopy (TEM) image of the incommensurate triangular ($3-q$ modulated) phase of quartz. The black and white triangles correspond to domains with domain states $\mathbf{S}_1$ and $\mathbf{S}_2$, and the transition regions between black and white areas to domain walls (discommensurations). For a domain wall of a certain orientation there are no reversed domain walls with the same orientation but reversed order of black and white; the walls are, therefore, non-reversible. Domain walls in regions with regular triangular structures are related by 120 and 240° rotations about the z direction and carry parallel spontaneous polarizations (see text). Triangular structures in two regions (blocks) with different orientations of the triangles are related *e.g.* by 2_x and carry, therefore, antiparallel spontaneous polarizations and behave macroscopically as two ferroelectric domains with antiparallel spontaneous polarization. Courtesy of E. Snoeck, CEMES, Toulouse and P. Saint-Grégoire, Université de Toulon.

ture in which these six symmetry-related wall orientations still prevail (Van Landuyt *et al.*, 1985).

3.4.4.5. *Ferroelastic domain twins and walls. Ferroelastic twin laws*

As explained in Section 3.4.3.6, from a domain pair $(\mathbf{S}_1, \mathbf{S}_j)$ of ferroelastic single-domain states with two perpendicular equally deformed planes p and p' one can form four different ferroelastic twins (see Fig. 3.4.3.8). Two mutually reversed twins $(\mathbf{S}_1|\mathbf{n}|\mathbf{S}_j)$ and $(\mathbf{S}_j|\mathbf{n}|\mathbf{S}_1)$ have the same twin symmetry $\mathsf{T}_{1j}(p)$ and the same symmetry $\overline{\mathsf{J}}_{1j}(p)$ of the twin pair $(\mathbf{S}_1, \mathbf{S}_j|\mathbf{n}|\mathbf{S}_j, \mathbf{S}_1)$. The *ferroelastic twin laws* can be expressed by the layer group $\overline{\mathsf{J}}_{1j}(p)$ or, in a less complete way (without specification of reversibility), by the twin symmetry $\mathsf{T}_{1j}(p)$. The same holds for two mutually reversed twins $(\mathbf{S}_1|\mathbf{n}'|\mathbf{S}_j)$ and $(\mathbf{S}_j|\mathbf{n}'|\mathbf{S}_1)$ with a twin plane p' perpendicular to p.

Table 3.4.4.6 summarizes possible symmetries T_{1j} of ferroelastic domain twins and corresponding ferroelastic twin laws $\overline{\mathsf{J}}_{1j}$. Letters V and W signify strain-dependent and strain-independent (with a fixed orientation) domain walls, respectively. The classification of domain walls and twins is defined in Table 3.4.4.3. The last column contains twinning groups $K_{1j}(F_1)$ of ordered domain pairs $(\mathbf{S}_1, \mathbf{S}_j)$ from which these twins can be formed. The symbol of K_{1j} is followed by a symbol of the group F_1 given in square brackets. The twinning group $K_{1j}(F_1)$ specifies, up to two cases, a class of equivalent domain pairs [orbit $G(\mathbf{S}_1, \mathbf{S}_j)$] (see Section 3.4.3.4). More details on particular cases (orientation of domain walls, disorientation angle, twin axis) can be found in synoptic Table 3.4.3.6. From this table follow two general conclusions:

(1) All layer groups describing the symmetry of compatible ferroelastic domain walls are polar groups, therefore *all compatible ferroelastic domain walls in dielectric crystals can be spontaneously polarized*. The direction of the spontaneous polarization is parallel to the intersection of the wall plane p and the plane of shear (*i.e.* a plane perpendicular to the axis of the ferroelastic domain pair, see Fig. 3.4.3.5*b* and Section 3.4.3.6.2).

(2) *Domain twin* $(\mathbf{S}_1|\mathbf{n}|\mathbf{S}_j)$ *formed in the parent clamping approximation from a single-domain pair* $(\mathbf{S}_1, \mathbf{S}_j)$ *and the relaxed domain twin* $(\mathbf{S}_1^+|\mathbf{n}|\mathbf{S}_j^-)$ *with disoriented domain states have the same symmetry groups* T_{1j} and $\overline{\mathsf{J}}_{1j}$.

This follows from simple reasoning: all twin symmetries T_{1j} in Table 3.4.4.6 have been derived in the parent clamping approximation and are expressed by the orthorhombic group *mm*2 or by some of its subgroups. As shown in Section 3.4.3.6.2, the maximal symmetry of a mechanically twinned crystal is also *mm*2. An additional simple shear accompanying the lifting of the parent clamping approximation cannot, therefore, decrease the symmetry $\mathsf{T}_{1j}(p)$ derived in the parent clamping approximation. In a similar way, one can prove the statement for the group $\overline{\mathsf{J}}_{1j}(p)$ of the twin pairs $(\mathbf{S}_1, \mathbf{S}_j|\mathbf{n}|\mathbf{S}_j, \mathbf{S}_1)$ and $(\mathbf{S}_1^+, \mathbf{S}_j^-|\mathbf{n}|\mathbf{S}_j^-, \mathbf{S}_1^+)$.

3.4.4.6. *Domain walls of finite thickness – continuous description*

A domain wall of zero thickness is a geometrical construct that enabled us to form a twin from a domain pair and to find a layer group that specifies the *maximal symmetry* of that twin. However, real domain walls have a finite, though small, thickness. Spatial changes of the structure within a wall may, or may not, lower the wall symmetry and can be conveniently described by a *phenomenological theory*.

We shall consider the simplest case of a one nonzero component η of the order parameter (see Section 3.1.2). Two nonzero equilibrium homogeneous values of $-\eta_0$ and $+\eta_0$ of this parameter correspond to two domain states $\mathbf{S}_1$ and $\mathbf{S}_2$. Spatial changes of the order parameter in a domain twin $(\mathbf{S}_1|\mathbf{n}|\mathbf{S}_2)$ with a zero-thickness domain wall are described by a step-like function $\eta(\xi) = -\eta_0$ for $\xi < 0$ and $\eta(\xi) = +\eta_0$ for $\xi > 0$, where ξ is the distance from the wall of zero thickness placed at $\xi = 0$.

A domain wall of finite thickness is described by a function $\eta(\xi)$ with limiting values $-\eta_0$ and η_0:

$$\lim_{\xi\to-\infty} \eta(\xi) = -\eta_0, \quad \lim_{\xi\to+\infty} \eta(\xi) = \eta_0. \tag{3.4.4.23}$$

If the wall is symmetric, then the profile $\eta(\xi)$ in one half-space, say $\xi < 0$, determines the profile in the other half-space $\xi > 0$. For continuous $\eta(\xi)$ fulfilling conditions (3.4.4.23) this leads to the condition

$$\eta(\xi) = -\eta(-\xi), \tag{3.4.4.24}$$

i.e. $\eta(\xi)$ must be an odd function. This requirement is fulfilled if there exists a non-trivial symmetry operation of a domain wall (twin): a side reversal ($\xi \to -\xi$) combined with an exchange of domain states [$\eta(\xi) \to -\eta(\xi)$] results in an identical wall profile.

A particular form of the wall profile $\eta(\xi)$ can be deduced from Landau theory. In the simplest case, the dependence $\eta(\xi)$ of the domain wall would minimize the free energy

$$\int_{-\infty}^{\infty} \left(\Phi_0 + \tfrac{1}{2}\alpha(T - T_c)\eta^2 + \tfrac{1}{4}\beta\eta^4 + \tfrac{1}{2}\delta\left(\frac{d^2\eta}{d\xi^2}\right)^2 \right) \mathrm{d}\xi, \tag{3.4.4.25}$$

where α, β, δ are phenomenological coefficients and T and T_c are the temperature and the temperature of the phase transition, respectively. The first three terms correspond to the homogeneous part of the Landau free energy (see Section 3.2.1) and the last term expresses the energy of the spatially changing order parameter. This variational task with boundary conditions (3.4.4.23) has the following solution (see *e.g.* Salje, 1990, 2000*b*; Ishibashi, 1990; Strukov & Levanyuk, 1998)

$$\eta(\xi) = \eta_0 \tanh(\xi/w), \tag{3.4.4.26}$$

where the value w specifies one half of the *effective thickness* $2w$ *of the domain wall* and is given by

Table 3.4.4.6. *Symmetry properties of ferroelastic domain twins and compatible domain walls*

T_{1j}	$\overline{\mathsf{J}}_{1j}$	Classification		$K_{1j}[F_1]$
1	$\underline{2}$	V	A$\underline{\mathrm{R}}$	$4^\star[2]$, $\bar{4}^\star[2]$, 6[2], $6/m[2]$
1	$\underline{2}$	V	A$\underline{\mathrm{R}}$	
1	$2^\star$	W	AR*	$2^\star[1]$, 422[2], $\bar{4}2m[m]$, 32[2], $\bar{3}m[m]$, 622[2], $\bar{6}m2[m]$, 432[222], $m\bar{3}m[mm2]$, $m\bar{3}m[2^\star_{xy}][mm2]$
$\underline{2}^\star$	$\underline{2}^\star$	V	SI	
1	$2^\star$	W	AR*	23[3], 432[4], 432[3], $m\bar{3}m[\bar{4}]$
$\underline{2}^\star$	$\underline{2}^\star$	W	SI	
1	$m^\star$	V	AR*	$m^\star[1]$, $4mm[m]$, $\bar{4}2m[2]$, $3m[m]$, $\bar{3}m[2]$, $6mm[m]$, $\bar{6}m2[2]$, $43m[mm2]$, $m\bar{3}m[222]$, $m\bar{3}m[m^\star_{xy}][m2m]$
$\underline{m}^\star$	$\underline{m}^\star$	W	SI	
1	$m^\star$	W	AR*	$m\bar{3}[3]$, $\bar{4}3m[\bar{4}]$, $\bar{4}3m[3]$, $m\bar{3}m[4]$
$\underline{m}^\star$	$\underline{m}^\star$	W	SI	
$\underline{2}^\star$	$2^\star\underline{2}^\star\underline{2}$	W	SR	$2^\star2^\star2[2]$, $4^\star22^\star[222]$, $\bar{4}^\star2^\star m[mm2]$, 622[222], $6/mmm[mm2]$, 432[422], 432[32], $m\bar{3}m[\bar{4}2m]$
$\underline{2}^\star$	$\underline{2}^\star2^\star\underline{2}$	W	SR	
$\underline{2}^\star$	$\underline{2}^\star/m^\star$	V	SR	$2^\star/m^\star[\bar{1}]$, $4/mmm[2/m]$, $\bar{3}m[2/m]$, $6/mmm[2/m]$, $m\bar{3}m[mmm]$
$\underline{m}^\star$	$2^\star/\underline{m}^\star$	W	SR	
$\underline{2}^\star$	$\underline{2}^\star/m^\star$	W	SR	$m\bar{3}[\bar{3}]$, $m\bar{3}m[4/m]$, $m\bar{3}m[\bar{3}]$
$\underline{m}^\star$	$2^\star/\underline{m}^\star$	W	SR	
m	m	V	AI	$4/m[m]$, $\bar{6}[m]$, $6/m[m]$
m	m	V	AI	
m	$\underline{2}/m$	V	A$\underline{\mathrm{R}}$	$4^\star/m[2/m]$, $6/m[2/m]$
m	$\underline{2}/m$	V	A$\underline{\mathrm{R}}$	
$\underline{m}^\star$	$m^\star\underline{m}^\star\underline{2}$	W	SR	$m^\star m^\star2[2]$, $4^\star mm^\star[mm2]$, $\bar{4}^\star2m^\star[222]$, $6mm[mm2]$, $6/mmm[222]$, $43m[\bar{4}2m]$, $m\bar{3}m[422]$, $m\bar{3}m[32]$
$\underline{m}^\star$	$\underline{m}^\star m^\star\underline{2}$	W	SR	
m	$m^\star2^\star m$	W	AR*	$m^\star2^\star m[m]$, $4/mmm[2mm]$, $\bar{6}m2[m2m]$, $6/mmm[m2m]$, $\bar{4}3m[3m]$, $m\bar{3}m[4mm]$, $m\bar{3}m[\bar{4}2m]$, $m\bar{3}m[3m]$
$\underline{m}^\star\underline{2}^\star m$	$\underline{m}^\star\underline{2}^\star m$	W	SI	
$\underline{m}^\star\underline{2}^\star m$	$\underline{m}^\star m^\star m$	W	SR	$m^\star m^\star m[2/m]$, $4^\star/mmm^\star[mmm]$, $6/mmm[mmm]$, $m\bar{3}m[4/mmm]$, $m\bar{3}m[\bar{3}m]$
$2^\star\underline{m}^\star m$	$m^\star\underline{m}^\star m$	W	SR	

$$w = \sqrt{2\delta/\alpha(T_c - T)}. \qquad (3.4.4.27)$$

This dependence, expressed in relative dimensionless variables ξ/w and η/η_0, is displayed in Fig. 3.4.4.6.

The wall profile $\eta(\xi)$ expressed by solution (3.4.4.26) is an odd function of ξ,

$$\eta(-\xi) = \eta_0 \tanh(-\xi/w) = -\eta_0 \tanh(\xi/w) = -\eta(\xi), \qquad (3.4.4.28)$$

and fulfils thus the condition (3.4.4.24) of a symmetric wall.

The wall thickness can be estimated from electron microscopy observations, or more precisely by a diffuse X-ray scattering technique (Locherer *et al.*, 1998). The effective thickness $2w$ [see equation (3.4.4.26)] in units of crystallographic repetition length A normal to the wall ranges from $2w/A = 2$ to $2w/A = 12$, *i.e.* $2w$ is about 10–100 nm (Salje, 2000*b*). The temperature dependence of the domain wall thickness expressed by equation (3.4.4.27) has been experimentally verified, *e.g.* on $LaAlO_3$ (Chrosch & Salje, 1999).

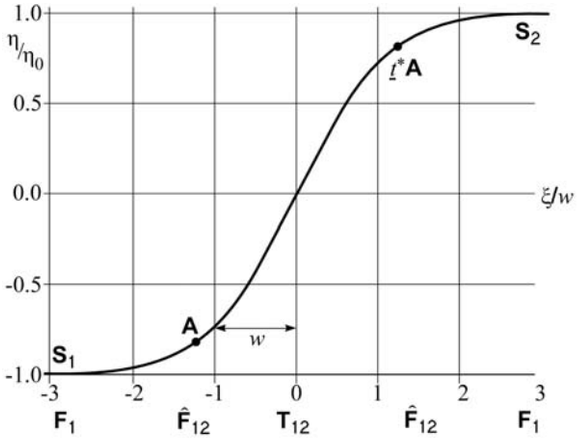

Fig. 3.4.4.6. Profile of the one-component order parameter $\eta(\xi)$ in a symmetric wall (S). The effective thickness of the wall is $2w$.

The energy σ of the domain wall per unit area equals the difference between the energy of the twin and the energy of the single-domain crystal. For a one nonzero component order parameter with the profile (3.4.4.26), the wall energy σ is given by (Strukov & Levanyuk, 1998)

$$\sigma = \int_{-\infty}^{\infty} \big[\Phi(\eta(\xi)) - \Phi(\eta_0)\big]\,\mathrm{d}\xi = \frac{2\sqrt{2\delta}}{3\beta}[\alpha(T_c - T)]^{3/2}, \qquad (3.4.4.29)$$

where $2w$ is the effective thickness of the wall [see equation (3.4.4.27)] and the coefficients are defined in equation (3.4.4.25).

The order of magnitude of the wall energy σ of ferroelastic and non-ferroelastic domain walls is typically several millijoule per square metre (Salje, 2000*b*).

Example 3.4.4.3. In our example of a ferroelectric phase transition $4_z/m_z m_x m_{xy} \supset 2_x m_y m_z$, one can identify η with the P_1 component of spontaneous polarization and ξ with the axis y. One can verify in Fig. 3.4.4.6 that the symmetry $\mathsf{T}_{12}[010] = \underline{2}^\star_z/m_z$ of the twin $(\mathbf{S}_1[010]\mathbf{S}_2)$ with a zero-thickness domain wall is retained in the domain wall with symmetric profile (3.4.4.26): both non-trivial symmetry operations $\underline{2}^\star_z$ and $\underline{1}^\star$ transform the profile $\eta(y)$ into an identical function.

This example illustrates another feature of a symmetric wall: All non-trivial symmetry operations of the wall are located at the central plane $\xi = 0$ of the finite-thickness wall. The sectional group T_{12} of this plane thus expresses the *symmetry of the central layer* and also the *global symmetry* of a symmetric wall (twin). The *local symmetry* of the off-centre planes $\xi \neq 0$ is equal to the face group $\widehat{\mathsf{F}}_{12}$ of the the layer group T_{12} (in our example $\widehat{\mathsf{F}}_{12} = \{1, m_z\}$).

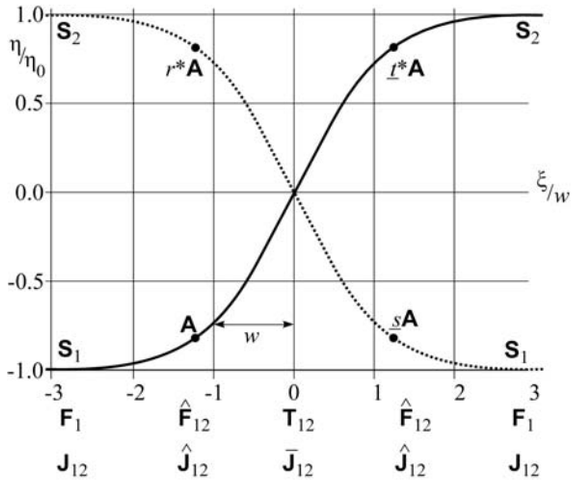

Fig. 3.4.4.7. Profiles of the one-component order parameter $\eta(\xi)$ in a symmetric wall (solid curve) and in the reversed wall (dotted curve). The wall is symmetric and reversible (SR).

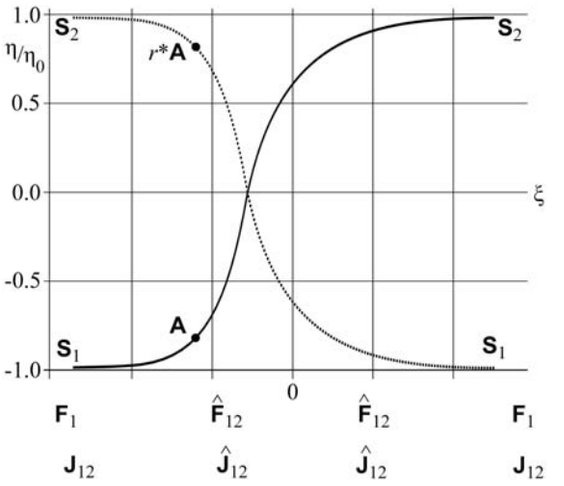

Fig. 3.4.4.8. Profiles of the one-component order parameter $\eta(\xi)$ in an asymmetric wall (solid curve) and in the reversed asymmetric wall (dotted curve). The wall is asymmetric and state-reversible (AR*).

The relation between a wall profile $\eta(\xi)$ of a *symmetric reversible* (SR) *wall* and the profile $\eta^{\rm rev}(\xi)$ of the reversed wall is illustrated in Fig. 3.4.4.7, where the the dotted curve is the wall profile $\eta^{\rm rev}(\xi)$ of the reversed wall. The profile $\eta^{\rm rev}(\xi)$ of the reversed wall is completely determined by the the profile $\eta(\xi)$ of the initial wall, since both profiles are related by equations

$$\eta^{\rm rev}(\xi) = -\eta(\xi) = \eta(-\xi). \qquad (3.4.4.30)$$

The first part of the equation corresponds to a state-exchanging operation $r^{\star}_{12}$ (*cf.* point $r^{\star}$A in Fig. 3.4.4.7) and the second one to a side-reversing operation $\underline{s}_{12}$ (point $\underline{s}$A in the same figure). In a symmetric reversible wall, both types of reversing operations exist (see Table 3.4.4.3).

In a *symmetric irreversible* (SI) *wall* both initial and reversed wall profiles fulfil symmetry condition (3.4.4.24) but equations (3.4.4.30) relating both profiles do not exist. The profiles $\eta(\xi)$ and $\eta^{\rm rev}(\xi)$ may differ in shape and surface wall energy. Charged domain walls are always irreversible.

A possible profile of an *asymmetric domain wall* is depicted in Fig. 3.4.4.8 (full curve). There is no relation between the negative part $\eta(\xi) < 0$ and positive part $\eta(\xi) > 0$ of the wall profile $\eta(\xi)$. Owing to the absence of non-trivial twin operations, there is no central plane with higher symmetry. The local symmetry (sectional layer group) at any location ξ within the wall is equal to the face group $\widehat{\mathsf{F}}_{12}$. This is also the global symmetry T_{12} of the entire wall, $\mathsf{T}_{12} = \widehat{\mathsf{F}}_{12}$.

The dotted curve in Fig. 3.4.4.8 represents the reversed-wall profile of an *asymmetric state-reversible* (AR*) *wall* that is related to the initial wall by state-exchanging operations $r^{\star}_{12}\widehat{\mathsf{F}}_{12}$ (see Table 3.4.4.5),

$$\eta^{\rm rev}(\xi) = -\eta(\xi). \qquad (3.4.4.31)$$

An example of an *asymmetric side-reversible* (A$\underline{\rm R}$) *wall* is shown in Fig. 3.4.4.9. In this case, an asymmetric wall (full curve) and reversed wall (dotted curve) are related by side-reversing operations $\underline{s}_{12}\widehat{\mathsf{F}}_{12}$:

$$\eta^{\rm rev}(\xi) = \eta(-\xi). \qquad (3.4.4.32)$$

In an *asymmetric irreversible* (AI) *wall*, both profiles $\eta(\xi)$ and $\eta^{\rm rev}(\xi)$ are asymmetric and there is no relation between these two profiles.

The *symmetry* $\mathsf{T}_{12}(\eta)$ *of a finite-thickness wall* with a profile $\eta(\xi)$ is equal to or lower than the symmetry T_{12} of the corresponding zero-thickness domain wall, $\mathsf{T}_{12} \supseteq \mathsf{T}_{12}(\eta)$. A symmetry descent $\mathsf{T}_{12} \supset \mathsf{T}_{12}(\eta)$ can be treated as a phase transition in the domain wall (see *e.g.* Bul'bich & Gufan, 1989*a*,*b*; Sonin & Tagancev, 1989). There are $n_{W(\eta)}$ equivalent *structural variants of the finite-thickness domain wall* with the same orientation and the same energy but with different structures of the wall,

$$n_{W(\eta)} = [\mathsf{T}_{12} : \mathsf{T}_{12}(\eta)] = |\mathsf{T}_{12}| : |\mathsf{T}_{12}(\eta)|. \qquad (3.4.4.33)$$

Domain-wall variants – two-dimensional analogues of domain states – can coexist and meet along line defects – one-dimensional analogues of a domain wall (Tagancev & Sonin, 1989).

Symmetry descent in domain walls of finite thickness may occur if the order parameter η has more than one nonzero component. We can demonstrate this on ferroic phases with an order parameter with two components η_1 and η_2. The profiles $\eta_1(\xi)$ and $\eta_2(\xi)$ can be found, as for a one-component order parameter, from the corresponding Landau free energy (see *e.g.* Cao & Barsch, 1990; Houchmandzadeh *et al.*, 1991; Ishibashi, 1992, 1993; Rychetský & Schranz, 1993, 1994; Schranz, 1995; Huang *et al.*, 1997; Strukov & Levanyuk, 1998; Hatt & Hatch, 1999; Hatch & Cao, 1999).

Let us denote by $\mathsf{T}_{12}(\eta_1)$ the symmetry of the profile $\eta_1(\xi)$ and by $\mathsf{T}_{12}(\eta_2)$ the symmetry of the profile $\eta_2(\xi)$. Then the symmetry of the entire wall $\mathsf{T}_{12}(\eta)$ is a common part of the symmetries $\mathsf{T}_{12}(\eta_1)$ and $\mathsf{T}_{12}(\eta_2)$,

$$\mathsf{T}_{12}(\eta) = \mathsf{T}_{12}(\eta_1) \cap \mathsf{T}_{12}(\eta_2). \qquad (3.4.4.34)$$

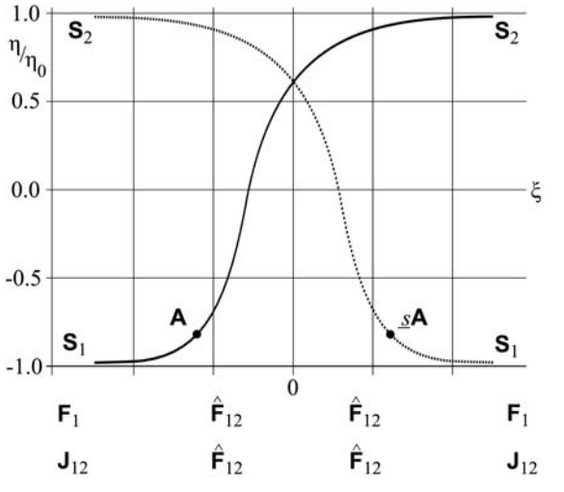

Fig. 3.4.4.9. Profiles of the one-component order parameter $\eta(\xi)$ in an asymmetric wall (solid curve) and in the reversed asymmetric wall (dotted curve). The wall is asymmetric and side-reversible (A$\underline{\rm R}$).

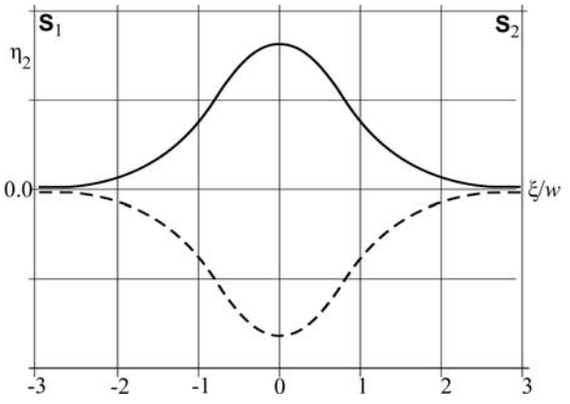

Fig. 3.4.4.10. A profile of the second order parameter component in a degenerate domain wall.

Example 3.4.4.4. In our illustrative phase transition $4_z/m_z m_x m_{xy} \supset 2_x m_y m_z$, the order parameter has two components η_1, η_2 that can be associated with the x and y components P_1 and P_2 of the spontaneous polarization (see Table 3.1.3.1 and Fig. 3.4.2.2). We have seen that the domain wall $[\mathbf{S}_1[010]\mathbf{S}_2]$ of zero thickness has the symmetry $\mathsf{T}_{12} = \underline{2}^\star_z/m_z$. If one lets $\eta_1(y)$ relax and keeps $\eta_2(y) = 0$ (a so-called *linear structure*), then $\mathsf{T}_{12}(\eta_1) = \underline{2}^\star_z/m_z$ (see Fig. 3.4.4.2 with $\xi = y$). If the last condition is lifted, a possible profile of a relaxed $\eta_2(y)$ is depicted by the full curve in Fig. 3.4.4.10. If both components $\eta_1(y)$ and $\eta_2(y)$ are nonzero within the wall, one speaks about a *rotational structure* of domain wall. In this relaxed domain wall the spontaneous polarization rotates in the plane (001), resembling thus a Néel wall in magnetic materials. The even profile $\eta_2(-y) = \eta_2(y)$ has the symmetry $\mathsf{T}_{12}(\eta_2) = m^\star_x 2^\star_y m_z$. Hence, according to (3.4.4.34), the symmetry of a relaxed wall with a rotational structure is $\mathsf{T}_{12}(\eta) = \underline{2}^\star_z/m_z \cap m^\star_x 2^\star_y m_z = \{1, m_z\}$. This is an asymmetric state-reversible ($\mathrm{AR}^\star$) wall with two chiral variants [see equation (3.4.4.33)] that are related by $\underline{\bar{1}}^\star$ and $\underline{2}^\star_z$; the profile $\eta_2(y)$ of the second variant is depicted in Fig. 3.4.4.10 by a dashed curve.

Similarly, one gets for a zero-thickness domain wall $[\mathbf{S}_1[001]\mathbf{S}_2]$ perpendicular to z the symmetry $\mathsf{T}_{12} = \underline{2}^\star_y/m_y$. For a relaxed domain wall with profiles $\eta_1(z)$ and $\eta_2(z)$, displayed in Figs. 3.4.4.6 and 3.4.4.10 with $\xi = z$, one gets $\mathsf{T}_{12}(\eta_1) = \underline{2}^\star_y/m_y$, $\mathsf{T}_{12}(\eta_2) = m^\star_x \underline{2}^\star_y m_z$ and $\mathsf{T}_{12}(\eta) = \{1, \underline{2}^\star_y\}$. The relaxed domain wall with rotational structure has lower symmetry than the zero-thickness wall or the wall with linear structure, but remains a symmetric and reversible (SR) domain wall in which spontaneous polarization rotates in a plane (001), resembling thus a Bloch wall in magnetic materials. Two chiral right-handed and left-handed variants are related by operations m_z and $\underline{\bar{1}}^\star$. This example illustrates that the structure of domain walls may differ with the wall orientation.

We note that the stability of a domain wall with a rotational structure and with a linear structure depends on the values of the coefficients in the Landau free energy, on temperature and on external fields. In favourable cases, a phase transition from a symmetric linear structure to a less symmetric rotational structure can occur. Such phase transitions in domain walls have been studied theoretically by Bul'bich & Gufan (1989*a*,*b*) and by Sonin & Tagancev (1989).

3.4.4.7. *Microscopic structure and symmetry of domain walls*

The thermodynamic theory of domain walls outlined above is efficient in providing quantitative results (wall thickness, energy) in any specific material. However, since this is a continuum theory, it is not able to treat local structural changes on a microscopic level and, moreover, owing to the small thickness of domain walls (several lattice constants), the reliability of its conclusions is to some extent uncertain.

Discrete theories either use simplified models [*e.g.* pseudospin ANNNI (axial next nearest neighbour Ising) model] that yield quantitative results on profiles, energies and interaction energies of walls but do not consider real crystal structures, or calculate numerically for a certain structure the atomic positions within a wall from interatomic potentials.

Symmetry analysis of domain walls provides useful qualitative conclusions about the microscopic structure of walls. Layer groups with discrete two-dimensional translations impose, *via* the site symmetries, restrictions on possible displacements and/or ordering of atoms or molecules. From these conclusions, combined with a reasonable assumption that these shifts or ordering vary continuously within a wall, one gets *topological constraints on the field of local displacements and/or ordering of atoms or molecules in the wall*. The advantage of this treatment is its simplicity and general validity, since no approximations or simplified models are needed. The analysis can also be applied to domain walls of zero thickness, where thermodynamic theory fails. However, this method does not yield any quantitative results, such as values of displacements, wall thickness, energy *etc*.

The procedure is similar to that in the continuum description. The main relations equations (3.4.4.12)–(3.4.4.17) and the classification given in Table 3.4.4.3 hold for a microscopic description as well; one has only to replace point groups by space groups.

A significant difference is that the sectional layer groups and the wall symmetry depend on the location of the plane p in the crystal lattice. This position can by expressed by a vector $s\mathbf{d}$, where $\mathbf{d}$ is the *scanning vector* (see *IT* E, 2010 and the example below) and s is a non-negative number smaller than 1, $0 \le s < 1$. An extended symbol of a twin in the microscopic description, corresponding to the symbol (3.4.4.1) in the continuum description, is

$$(\mathsf{S}_1|\mathbf{n}; s\mathbf{d}|\mathsf{S}_2) \equiv (\mathsf{S}_2|-\mathbf{n}; s\mathbf{d}|\mathsf{S}_1). \qquad (3.4.4.35)$$

The main features of the analysis are demonstrated on the following example.

Example 3.4.4.5. Ferroelastic domain wall in calomel. We examine a ferroelastic compatible domain wall in a calomel crystal (Janovec & Zikmund, 1993; *IT* E, 2010, Chapter 5.2). In Section 3.4.2.5, Example 3.4.2.7, we found the microscopic domain states (see Fig. 3.4.2.5) and, in Section 3.4.3.7, the corresponding ordered domain pair $(\mathsf{S}_1, \mathsf{S}_3)$ and unordered domain pair $\{\mathsf{S}_1, \mathsf{S}_3\}$ (depicted in Fig. 3.4.3.10). These pairs have symmetry groups $\mathcal{F}_{13} = Pn_{x\bar{y}}n_{xy}m_z$ and $\mathcal{J}_{13} = P4^\star_{2z}/m_z n_{xy} m^\star_x$, respectively. Both groups have an orthorhombic basis $\mathbf{a}^o = \mathbf{a}^t - \mathbf{b}^t$, $\mathbf{b}^o = \mathbf{a}^t + \mathbf{b}^t$, $\mathbf{c}^o = \mathbf{c}^t$, with a shift of origin $\mathbf{b}^t/2$ for both groups.

Compatible domain walls in this ferroelastic domain pair have orientations (100) and (010) in the tetragonal coordinate system (see Table 3.4.3.6). We shall examine the former case – the latter is crystallographically equivalent. Sectional layer groups of this plane in groups $\mathcal{F}_{13}$ and $\mathcal{J}_{13}$ have a two-dimensional translation group (net) with basic vectors $\mathbf{a}^s = 2\mathbf{b}^t$ and $\mathbf{b}^s = \mathbf{c}^t$, and the scanning vector $\mathbf{d} = 2\mathbf{a}^t$ expresses the repetition period of the layer structure (*cf.* Fig. 3.4.3.10*a*). From the diagram of symmetry elements of the group $\mathcal{F}_{13}$ and $\mathcal{J}_{13}$, available in *IT* A (2005), one can deduce the sectional layer groups at any location $s\mathbf{d}$, $0 \le s < 1$. These sectional layer groups are listed explicitly in *IT* E (2010) in the *scanning tables* of the respective space groups.

The resulting sectional layer groups $\overline{\mathcal{F}}_{13}$ and $\overline{\mathcal{J}}_{13}$ are given in Table 3.4.4.7 in two notations, in which the letter p signifies a two-dimensional net with the basic translations $\mathbf{a}^s$, $\mathbf{b}^s$ introduced above. Standard symbols are related to the basis $\mathbf{a}^s$, $\mathbf{b}^s$, $\mathbf{c}^s = \mathbf{d}$. Subscripts in non-coordinate notation specify the orientation of symmetry elements in the reference Cartesian coordinate system of the tetragonal phase, the partial translation in the glide plane a and in the screw axis 2_1 is equal to $\frac{1}{2}\mathbf{a}^s = \mathbf{b}^t$, *i.e.* the symbols a and 2_1 are also related to the basis $\mathbf{a}^s$, $\mathbf{b}^s$, $\mathbf{c}^s$. At special locations $s\mathbf{d} = 0\mathbf{d}$, $\frac{1}{2}\mathbf{d}$ and $s\mathbf{d} = \frac{1}{4}\mathbf{d}$, $\frac{3}{4}\mathbf{d}$, sectional groups contain both side-